Electron density depletion: A case study

Author: Carlos Iglesias Mac-Cragh.
*Facultat de Física, Universitat de Barcelona, Diagonal 645, 08028 Barcelona, Spain.**

UB supervisor: Pilar Neus Queralt
UNIS supervisor: Lindis Bjoland

Abstract: This paper reviews what is known from other studies about electron density depletion regions found in polar regions and discusses about the different factors that can contribute to the formation of these structures. Using specific data from the EISCAT Svalbard radar, located around 78°N, extended in different seasons of 2007, it has been confirmed most of the statistical observations of other studies from longer periods of time and a possible relation between the occurrence of depletions and some of the solar wind parameters has been found. Due to the lack of available data, not enough statistical data treatment has been done to reinforce the formulated hypothesis, therefore, future studies should be able to manage bigger amount of data.

I. INTRODUCTION

Electron density depletion regions are plasma structures, mainly located on the F-layer of the ionosphere, in which the electron density is reduced far below the mean daily value. While several studies have been carried out at low and mid latitudes, there are fewer of them focusing on polar regions. Study these structures at high latitudes, where the ionosphere it is strongly conditioned by the solar wind influence, would provide a better comprehension of the Earth ionosphere-magnetosphere coupled system.

There are many different processes that can affect the electron density on the ionosphere. When it comes to production, the main mechanisms are related with ionization by solar radiation and by particle precipitation during geomagnetic events. Electron loss is, in general, due to recombination with ionic Oxygen (O_2^+) and Nitrogen Monoxide (NO^+) present at these ionospheric altitudes. Therefore, ionospheric electron density has a strong dependence with those variables playing a role on the ionization and recombination rates, like daily and seasonal variation of solar illumination and thermospheric composition, periods of solar activity, and the solar cycle itself. Recombination in the F-region usually takes place in a series of two-step reactions (e.g., Rodger et al., 1992; Schunk et al., 1976):

$$\begin{aligned} O^+ + O_2 &\rightarrow O_2^+ + O \\ O^+ + N_2 &\rightarrow NO^+ + N \\ N_2^+ + O &\rightarrow NO^+ + N \\ N_2^+ + O_2 &\rightarrow N_2 + O_2^+ \end{aligned} \tag{1}$$

that produces O_2^+ and NO^+, that recombine with e^- to create neutral N_2 and O_2.

In general, depletion structures can be classified within three different categories: Ionospheric (mid or high latitude) troughs, polar holes and auroral cavities. Mid latitude troughs and polar holes formation mechanisms are due to the lack of sources of ionization during long periods of time, thus, while mid latitude troughs forms when certain region in the convection circulation gets stagnated in darkness, polar holes are related to circulation in prolongated darkness, when the geomagnetic activity is quite low, and the polar cusp gets enough contracted to allow circulation in dark conditions (Brinton et al., 1978; Jenner et al., 2020; Sojka et al., 1981). Formation of auroral cavities is controlled by downward field aligned currents, electron precipitation causes an upward flow of molecular ions into the F-region that increases the recombination rates (Voiculescu et al., 2016). When it comes to high latitude troughs, they tend to form when there is a big difference between neutral and ion velocities that will produce frictional heating (e.g., Jones et al., 1990), since increasing the ion temperature will have a direct effect on the recombination rates.

Bjoland et al. (2020) statistically studied the occurrence of these structures in the polar region above Svalbard, using data from the EISCAT Svalbard Radar (ESR) extended over several decades, and clearly observed that these polar depletion regions mainly take place during the morning time. This could be seen for all seasons and for every level of solar activity, except for the case of summer in periods of low solar activity. The phenomena is more often seen during equinoxes, while in summer tends to appear less, and weaker. In the same way, depletions seem stronger during high solar activity.

The present study pretends to review what is known about depletion regions, especially in the upper polar atmosphere, and to focus into more specific periods of time with minimum solar activity during 2007, the year with longer data availability. Based in the preliminary results, running an experiment with the ESR will be undertaken to try to find a depletion. With data from the EISCAT

*Electronic address: jiglesma11@alumnes.ub.edu

Svalbard radar, located at a latitude of 78° North, it is intended to find more specific correlations between the solar wind parameters, and the occurrence of depletion regions.

II. DATA AND METHODS

ESR is a magnetic field aligned 42 m antenna working at a frequency of 500 MHz located at 78.15° N, 16.03° E, around 10 km outside the Norwegian city of Longyearbyen, in the archipelago of Svalbard. Since the radar is not in operation mode most of the time, data close enough in time is barely available. Nonetheless, 2007 was the so called *polar year* and the radar was in operation for longer periods of time that allowed to study a specific set of dates rather than statistical data throughout the years.

Four sets of dates, corresponding to the four different seasons, have been studied. Table I shows the distribution of the selected dates. No distinction has been done between spring and autumn equinoxes. ESR makes measurements of some ionospheric parameters in an altitude range between 100 and 600 km. The electron density is expected to be maximum at altitudes of 300 km in years of solar minimum (Vickers et al., 2014).Thus, data from altitudes different than 300 km has been removed, ensuring data with better SNR. Measurements with quality factors $q \neq 0$ have been also removed to ensure greater reliability. Despite the daily variability of the ionospheric parameters, data fulfilling $|\overline{N_e} - N_e| > 3\sigma$, being $\overline{N_e}$ and σ the daily mean and standard deviation, have been considered as outliers and therefore, removed.

Together with the ESR data, solar wind measurements from the *ACE/DSCOVR* satellites have been also included in the study. This data has been time-shifted to the Earth's bow shock, making it easier to detect its influence on the ionosphere. Data with some kind of missing values due to not accurate enough measurement, have been deleted. Both sets of data are integrated over 5 minutes measurements for better resolution.

Bjoland et al. (2020) establishes the criteria to numerically define a depletion as those areas in where $N_e < \overline{N_e} - \sigma$, thus, in this study, values of the electron density lower than the mean minus one standard deviation, extended during a relatively long period of time, have been considered depletions.

Based in the preliminary results on the depletions occurrence, an experiment with the ESR was designed and undertaken to study, if found, a new depletion. Finally, the chosen dates were 30 and 31 of March and the first of April, since it was found that March and April are the months with more depletions.

TABLE I: Selected dates according to season

Season	**Month**	**Days**
Equinox	March / October	12
Winter	February	5
Summer	August	5

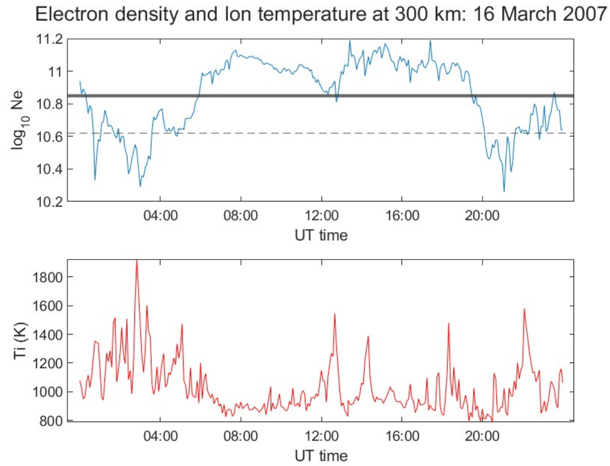

FIG. 1: Main ionospheric parameters as a function of UT time at an altitude of 300 km. On top: Electron density. At the bottom: Ion temperature. The wide black line represents the daily mean of the electron density, while the narrow dashed line represents the same mean minus a standard deviation.

III. RESULTS

Since this paper has been focused in studying sets of days, for each season of 2007, rather than in a statistical way, not all the resulting plots and graphics are shown in this paper. Just the most relevant for the purpose of the study are shown. The rest of them can be found in the *supplementary material*.

Figure 1 is a representative example of a depletion within all the analyzed cases. It is possible to clearly see a depletion region lasting approximately from 1 to 4 am in the morning sector, co-located with an enhancement in the ion temperature. Most of the analysed days containing depletions show the same tendency, depletions are usually co-located with high ion temperatures, that afterwards is reduced while the electron density increases again. Nonetheless, some of the dates seem to have depletions regions without a clear enhancement of the ion temperature and, in a similar way, some of the days have high ion temperatures without low electron densities at all. Table II shows that these structures are more likely to form during the equinoxes than in the other seasons. In addition, the depletions appear stronger during equinox and weaker during summer.

The most important parameters of the solar wind data are shown in figure 3. Comparing these plots with the electron density data, no clear correlation has been found

TABLE II: Occurrence of the depletions per season. March and October represents equinoxes regardless of if they are spring or autumn equinoxes. The column of *Depletions* represent the number of these found out of the total number of days analysed in that month, the mean electron density within each month can also be seen in the last column

Season	Month	depletions	$\overline{N_e}(/m^3)$
Equinox	March	4/6	$7.1 \cdot 10^{10}$
	October	5/6	$5.5 \cdot 10^{10}$
Winter	February	2/5	$3.7 \cdot 10^{10}$
Summer	August	1/5	$1.6 \cdot 10^{11}$

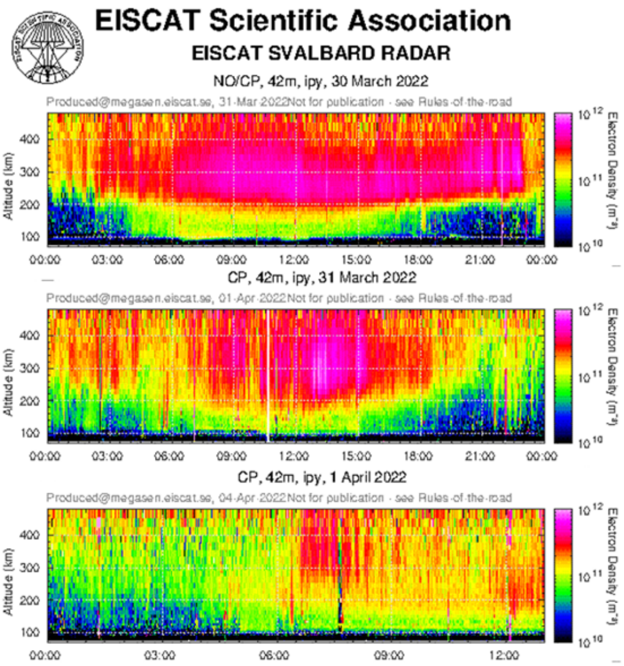

FIG. 2: Electron density profiles taken during the experiment at the EISCAT Svalbard radar. From top to bottom: 30 of March (whole day), 31 of March (whole day), 1 of April (half the day).

between the electron density and the solar wind flow speed, proton density or geomagnetic kp index. When it comes to the IMF, some regions seem to match with the electron density: When B_y and/or B_z becomes negative, the electron density seems to decrease, while when it gets positive, it happens the other way around.

Figure 2 shows the result of the experiment undertaken during this study at the ESR. While during the 31 of March, no depletion can be seen at first instance, during the next two days it is easy to spot them. What it seems a small depletion appears on the 31 of March around 4 am. During the 1^{st} of April, a strong depletion seem to appear from midnight until 6 am. Since the numeric data was not available yet on the release date of this paper, no numeric treatment of the data have been done. This should be done in order to confirm in a rigorous way the existence of depletions.

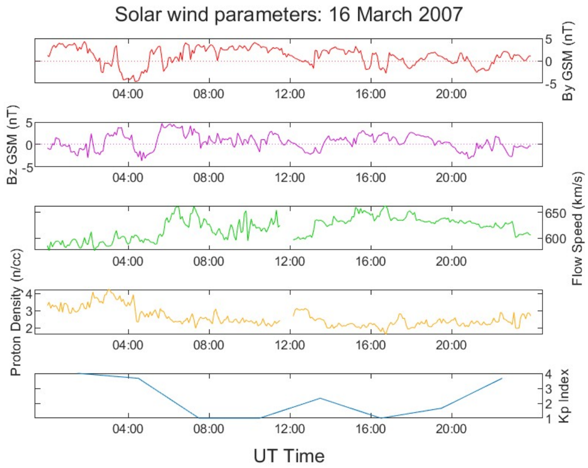

FIG. 3: Relevant solar wind parameters as a function of UT time for March 16^{th}, from top to bottom: y-component of the interplanetary magnetic field (IMF), z-component of the IMF, flow speed, proton density and *kp* index. Blank spaces represent missing data.

IV. DISCUSSION

From the three mechanisms of depletion formation, results from table I suggest that the main one could be related with ion frictional heating. If a higher occurrence of depletions were observed during the winter, could indicate that the formation mechanisms are related with prolonged recombination in darkness. Since polar holes and mid latitudes troughs are thought to be formed through stagnation of certain areas in the convection pattern when these are located in darkness and through circulation in darkness, these mechanisms would be suggested as the most likely ones. Nonetheless, the maximum seasonal occurrence of depletion happens during both equinoxes, when, according to Bjoland et al. (2020), the ionosphere at 300 km is sunlit during all the day. This might suggest that the most likely of them is the frictional heating. This is supported by figure 1, and many others, in which a depletion can be seen co-located with an increase of the ion temperature, that could most likely be caused by a strong frictional heating. However, as mentioned earlier, some of the results show an increase in the ion temperature that does not appear along with a decreased electron density. That suggests that ion frictional heating might not be the only mechanism taking part on the formation of these plasma structures.

The variations on the electron density that are seen within seasons may be due to changes on the ionospheric composition and the variation of the solar zenith angle. Solar zenith angle plays a role on the electron production rates, since more direct angles produce stronger ionization. Therefore, this is maximum in summer and minimum during winter, as can be seen in table II. In the other hand, ionospheric composition directly affects the rhythm at which reactions (1) take place, increasing or decreasing the recombination rates. The ionospheric composition comes primarily controlled by the meridional circulation from the summer hemisphere, where this circulation is flowing upwards, to the winter hemisphere, where it is flowing downwards. The rising flow in the summer hemisphere decreases the O to N_2 ratio, therefore enhancing recombination and decreasing the electron density. The sinking flow in the winter hemisphere, on the other side, causes a greater O/N_2 ratio, increasing the electron density in the winter hemisphere (Rishbeth, 1998). A combination of these factors might explain the seasonal differences on the electron density and the occurrence of depletions. For example, a much stronger production in summer would compensate for the losses due to recombination and would mask possible depletions. The combined effect would be proper for depletion formation during equinox.

The background ion temperature also plays a role in the rates of recombination reactions. During years of low solar minimum, like 2007, the solar activity is in general reduced in comparison with other parts of the solar cycle (Bjoland et al., 2020). Lower solar activity leads to a lower background ion temperature and thus, to less recombination. Could be that together with the strong ionization mentioned before, this background temperature could explain the lack of depletion occurrence seen in the results in summer.

It is possible that some of the parameters from the solar wind could have some kind of effect on the upper polar atmosphere, exposed to the IMF through periods of magnetic reconnection. It is expected that parameters like the proton density or the flow speed have certain effect on the geomagnetic activity, and thus, influence the electron density in the ionosphere. However, no clear evidence of that influence has been found during this study. This could be because 2007 was a solar minimum year and the solar activity was too low to cause visible effects during the chosen dates. Another possible explanation is that the number of available dates for this study is not enough. Further statistical studies trying to relate the occurrence of depletions with the different solar wind parameters would provide a better understanding on the specific role of the solar wind.

When it comes to the interplanetary magnetic field (IMF) components, some of the plots have shown a pattern between the latest and the electron density during the early morning. Figure 4 shows that the electron density decreases when the z component of the IMF does so, and increases again when this increases. This could actually be explained by the variations that the IMF induces on the convection pattern. When the the z component is negative, plasma in the ionosphere flows from the day-side to the night-side crossing the polar cap, while it returns within the auroral oval creating the classical two-cell convection circulation. As this component gets more negative, the auroral oval extends southwards and the cross polar cap potential increases (e.g. Reiff et al., 1981; Cowley, 1984; Weimer, 2001). That would cause the ion drift velocity to increase, producing more frictional heating and further recombination. The fact that this is only observed during early mornings could indicate that this effect gets masked by solar production when the solar zenith angle is great enough. Some of the figures, as can be seen in figure 5, also show this tendency with strong variations of the y component. This could be because B_y component causes the general convection pattern to twist clockwise or counterclockwise depending on its sign, and then, leading regions into the convection pattern that were not there before that twist. Being now inside a circulation region, would lead to a considerable increase on the ion frictional heating, and again, to a

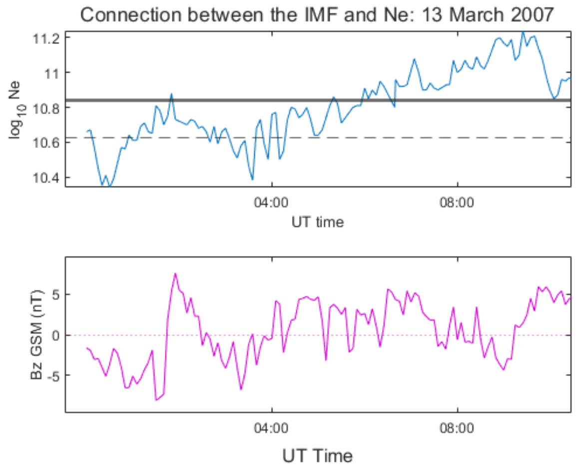

FIG. 4: Relation between the electron density (on top) and the z component of the IMF (at the bottom) during the early morning on the 13^{th} of March.

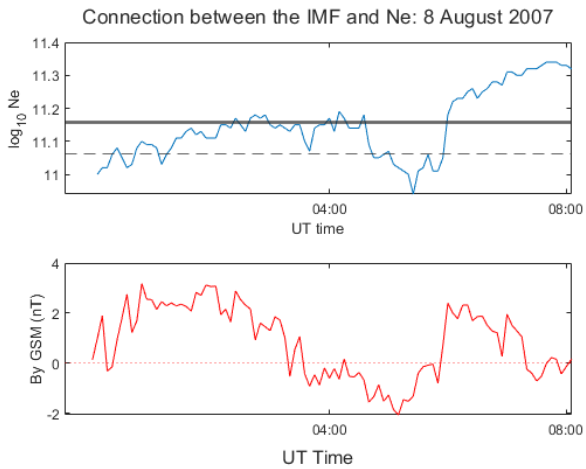

FIG. 5: Relation between the electron density (on top) and the y component of the IMF (at the bottom) during the early morning on the 8^{th} of August.

stronger recombination.

V. CONCLUSIONS

1. The results of this study confirm Bjoland et al. (2020) observations: depletions are more often seen in Equinox than in winter and summer. This could potentially be due to depletion formation due to frictional heating in polar regions.
2. Combined effects of the variation of the solar zenith angle and the ionospheric composition could explain seasonal variation of the electron density and depletion occurrence.
3. Depletions seem also be connected to the IMF components. However, further studies need to be conducted in order to consolidate these results and should be directed to better understand the role of the IMF on these kind of plasma structures and to find more correlations between the depletion structures and solar wind parameters.
4. Due to the lack of available data, not enough statistical data treatment has been done to reinforce the formulated hypothesis, therefore, future studies should be able to manage bigger amount of data.

Acknowledgments

I would like to thank:

Dr. Pilar Queralt for accepting my TFG proposal and Postdoc Lindis M. Bjoland for being my supervisor in Svalbard and guiding me through some of the steps.

Both institutions: Univeristat de Barcelona (UB) and The University Centre in Svalbard (UNIS) for making the agreement.

EISCAT scientific association and the staff at ESR for allowing us conducting the experiments.

My family for their economical support, and my friends at Longyearbyen, who helped me dealing with the polar night. Finally, to my partner, who helped me a lot throughout the process.

VI. REFERENCES

Bjoland, L. M., Ogawa, Y., Løvhaug, U. P., Lorentzen, D. A., Hatch, S. M., Oksavik, K. (2020). Electron density depletion region observed in the polar cap ionosphere. *Journal of Geophysical Research: Space Physics*, 126, e2020JA028432. https://doi.org/10.1029/2020JA028432

Brinton, H. C., Grebowsky, J. M., Brace, L. H. (1978). The high-latitude winter F region at 300 km: Thermal plasma observations from AE-C. *Journal of Geophysical Research*, 83(A10), 4767–4776. https://doi.org/10.1029/JA083iA10p04767

Cowley, S. W. H. (1984). Solar wind control of magnetospheric convection. Achievements of the International Magnetospheric Study (IMS), 217, 483.

Jenner, L. A., Wood, A. G., Dorrian, G. D., Oksavik, K., Yeoman, T. K., Fogg, A. R., et al. (2020). Plasma density gradients at the edge of polar ionospheric holes: the absence of phase scintillation. *Annales Geophysicae*, 38(2), 575–590. https://doi.org/10.5194/angeo-38-575-2020

Jones, G., Williams, P., Winser, K., Lockwood, M. (1990). Characteristics of the high-latitude trough. *Advances in Space Research*, 10(6), 191–196 https://doi.org/10.1016/0273-1177(90)90253-V

Reiff, P. H., Spiro, R. W., Hill, T. W. (1981). Dependence of polar cap potential drop on interplanetary parameters. *Journal of Geophysical Research: Space Physics*, 86(A9), 7639-7648.

Rishbeth, H. (1998). How the thermospheric circulation affects the ionospheric F2-layer. *Journal of Atmospheric and Solar-Terrestrial Physics*, 60(14), 1385–1402. https://doi.org/10.1016/S1364-6826(98)00062-5

Rodger, A., Moffett, R., Quegan, S. (1992). The role of ion drift in the formation of ionisation troughs in the mid- and high-latitude ionosphere—a review. *Journal of Atmospheric and Solar-Terrestrial Physics*, 54(1), 1–30. https://doi.org/10.1016/0021-9169(92)90082-V

Schunk, R. W., Banks, P. M., Raitt, W. J. (1976). Effects of electric fields and other processes upon the nighttime high-latitude F layer. *Journal of Geophysical Research*, 81(19), 3271–3282. https://doi.org/10.1029/JA081i019p03271

Sojka, J. J., Raitt, W. J., Schunk, R. W. (1981). Plasma density features associated with strong convection in the winter high-latitude F region. *Journal of Geophysical Research*, 86(A8), 6908–6916. https://doi.org/10.1029/JA086iA08p06908

Vickers, H., Kosch, M. J., Sutton, E., Bjoland, L., Ogawa, Y., La Hoz, C. (2014). A solar cycle of upper thermosphere density observations from the EISCAT Svalbard radar. *Journal of Geophysical Research: Space Physics*, 8(8), 6833–6845. https://doi.org/10.1002/2014JA019885

Voiculescu, M., Nygrén, T., Aikio, A. T., Vanhamäki, H., Pierrard, V. (2016). Postmidnight ionospheric troughs in summer at high latitudes. *Journal of Geophysical Research: Space Physics*, 121(12), 12171–12185. https://doi.org/10.1002/2016JA023360

Weimer, D. R. (2001). An improved model of ionospheric electric potentials including substorm perturbations and application to the Geospace Environment Modeling November 24, 1996, event. *Journal of Geophysical Research: Space Physics*, 106(A1), 407-416.